

Transparent magnetic semiconductors based on ZnO

This article has been downloaded from IOPscience. Please scroll down to see the full text article.

2004 J. Phys.: Condens. Matter 16 S5533

(<http://iopscience.iop.org/0953-8984/16/48/008>)

View [the table of contents for this issue](#), or go to the [journal homepage](#) for more

Download details:

IP Address: 129.252.86.83

The article was downloaded on 27/05/2010 at 19:16

Please note that [terms and conditions apply](#).

Transparent magnetic semiconductors based on ZnO

H Saeki, H Matsui, T Kawai and H Tabata

The Institute of Scientific and Industrial Research, Osaka University, 8-1 Mihogaoka, Ibaraki, Osaka 567-0047, Japan

Received 26 May 2004, in final form 17 August 2004

Published 19 November 2004

Online at stacks.iop.org/JPhysCM/16/S5533

doi:10.1088/0953-8984/16/48/008

Abstract

Transparent magnetic semiconductors have been constructed by introducing transition metals such as Co or V into wurtzite ZnO crystals by a non-equilibrium thin film technique using laser molecular beam epitaxy. Co and V substituted for Zn have a divalent cationic state in the ZnO thin films formed epitaxially on the sapphire substrates. Raman measurements show that the wurtzite crystal structure can be maintained up to 15% and 5% for Co and V substitution, respectively. The results from photoemission spectra also suggest that Co does not have a metal state but a 2+ state. Magnetic circular dichroism (MCD), x-ray MCD, superconducting quantum interference device (SQUID) and nuclear magnetic resonance (NMR) measurements on (Zn, Co)O films indicate ferromagnetic properties with magnetizations of 0.1–0.3 μ_B/Co .

(Some figures in this article are in colour only in the electronic version)

1. Introduction

Ferromagnetism in diluted magnetic semiconductors, especially transition-metal-doped wide-gap semiconductors [1–4], is currently a hot topic because of both applications to spintronics devices [5] and the desire to understand the mechanism of ferromagnetism. It is important to control both the electric properties and the magnetic properties of ZnO thin for practical applications in opto-electronic and opto-magnetic devices at room temperature. Recently it has been found, from superconducting quantum interference device (SQUID) measurements, that $\text{Zn}_{1-x}\text{Co}_x\text{O}$ and $\text{Zn}_{1-x}\text{V}_x\text{O}$ become room temperature ferromagnets upon doping with electrons [6, 7]. Although some research groups have reported considerable efforts to produce diluted magnetic semiconductors, fabrication of reliable practical devices operating at room temperature is subject to the limitations of low reproducibility and an unclear ferromagnetic mechanism. Therefore, it is desirable to realize reproducible transparent ferromagnetic semiconductors operating at room temperature.

ZnO is well known as a wide-band-gap semiconductor ($E_g = 3.3$ eV); furthermore, it has an exciton binding energy of 60 meV which is much higher than that at room temperature.

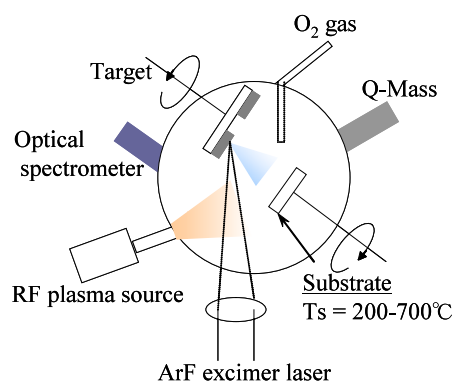


Figure 1. A schematic model of pulsed laser deposition.

Heterostructures and quantum wells can be fabricated using MgZnO and CdZnO acting as wide-gap and narrow-gap layers, respectively. Recently, many groups have reported on the electrical properties of ZnO films doped with impurities, such as Co [6] and N atoms [8, 9], from theoretical and experimental points of view. We have been aiming at fabricating quantum heterostructures confining spins and carriers to low-level sizes (one or two) using ZnO as the mother material.

2. Experimental details

Films with transition metal (TM) substituted for Zn in ZnO ($\text{Zn}_{1-x}\text{TM}_x\text{O}$ ($x = 0-0.50$)) were formed on $\alpha\text{-Al}_2\text{O}_3$ (0001) substrates using a pulsed laser deposition (PLD) technique (figure 1). A low-temperature process (non-equilibrium process) such as PLD is effective for introducing a much larger amount of exotic ions (magnetic ions) into the ZnO films, as compared with conventional synthesis processes for constructing bulk materials. Therefore, low-temperature formation enables us to introduce more exotic ions into ZnO than when using formation at high temperature. We found that a two-step growth approach was quite effective [10] for realizing the non-equilibrium process. Before forming the $\text{Zn}_{1-x}\text{TM}_x\text{O}$ layer, a pure ZnO layer (approximately 200 nm) was deposited at 600 °C in an oxygen atmosphere to obtain a well crystallized template layer. This seed layer is quite effective in improving the crystallinity and expanding the solubility limit. Then, the $\text{Zn}_{1-x}\text{TM}_x\text{O}$ layer was formed at relatively low temperature. All the $\text{Zn}_{1-x}\text{TM}_x\text{O}$ layers were formed at 340 °C in an oxygen ambient pressure from 10^{-5} to 10^{-4} Torr with a laser fluence of 1 J cm^{-2} . The deposition rate was $1-2 \text{ nm min}^{-1}$. A 1 min rapid thermal annealing (RTA) treatment was performed as a post-annealing process. The lattice parameter and crystal structures of the films were characterized by means of x-ray diffraction ($2\theta-\theta$ scanning) using a Cu $K\alpha$ source (Rigaku: RINT 2000). Magnetic measurements were performed using a SQUID magnetometer (Quantum Design MPMS-5S) with the magnetic field applied parallel to the film plane. The magnetic circular dichroism (MCD) and visible-UV spectra were measured using a JASCO 820-J under a magnetic field of -1.5 to $+1.5$ T. Nuclear magnetic resonance (NMR) measurements were performed by Kitaoka *et al* at Osaka University. XMCD, XAS and PES measurements were performed by Fujimori *et al* who are collaborators of ours.

3. Results and discussion

So far, one of the most serious problems in our experiments is that of lack of reproducibility. To overcome this, we treated the samples with a post-annealing process. In our experiments,

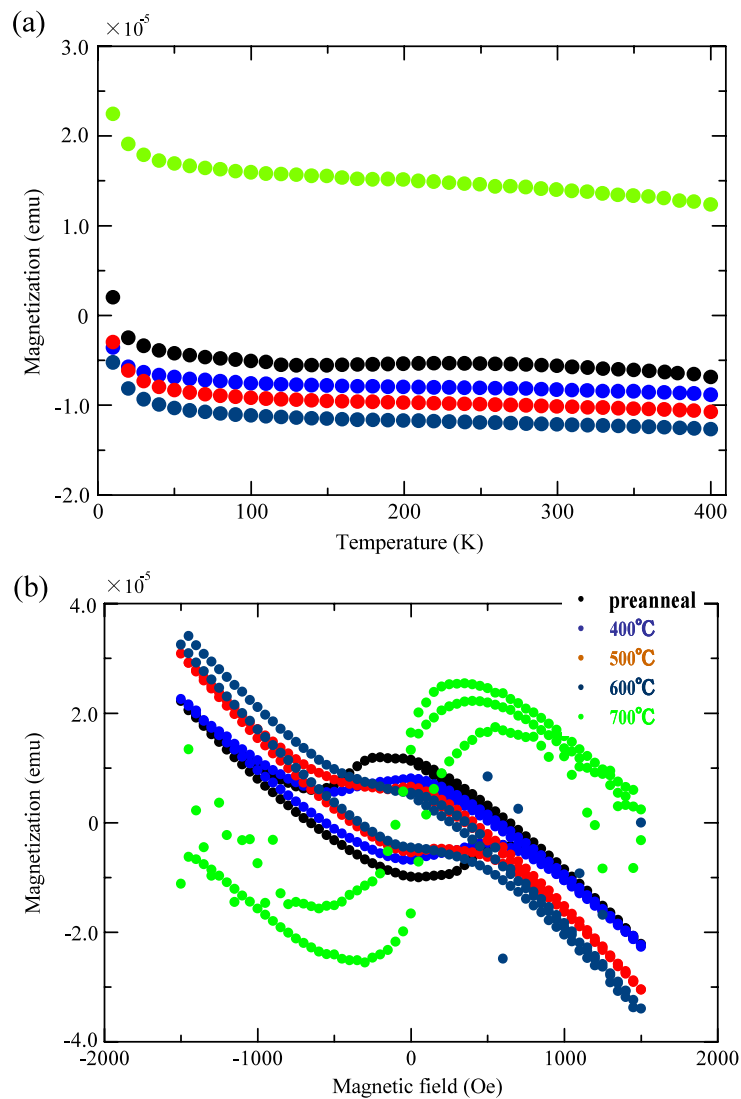


Figure 2. Temperature dependence of magnetization (a) and hysteresis curves (b) for ZnO:15% Co films, against the annealing temperature of the RTA for as-deposited films and ones following RTA at 400, 500, 600 and 700 °C.

we developed a rapid thermal annealing (RTA) system for post-treatment. It is effective for improving the crystallinity of the TM-doped ZnO films without generating third phases such as impurities and/or extracts. Figures 2(a) and (b) show the temperature and magnetic field dependence of the magnetization, against the annealing temperature of the RTA. As-deposited ZnO:Co film shows negative magnetization (figure 2(a)). $M-H$ hysteresis curves observed from SQUID measurements are improved with increasing annealing temperature. Eventually, typical ferromagnetic characteristics, such as positive magnetization and clear hysteresis properties, are observed after RTA treatment at 700 °C. A similar tendency is observed in the ZnO:V films (figure 3). In the case of ZnO:V films, a linear $M-H$ curve (paramagnetic properties) is observed for the as-deposited sample. After RTA treatment at

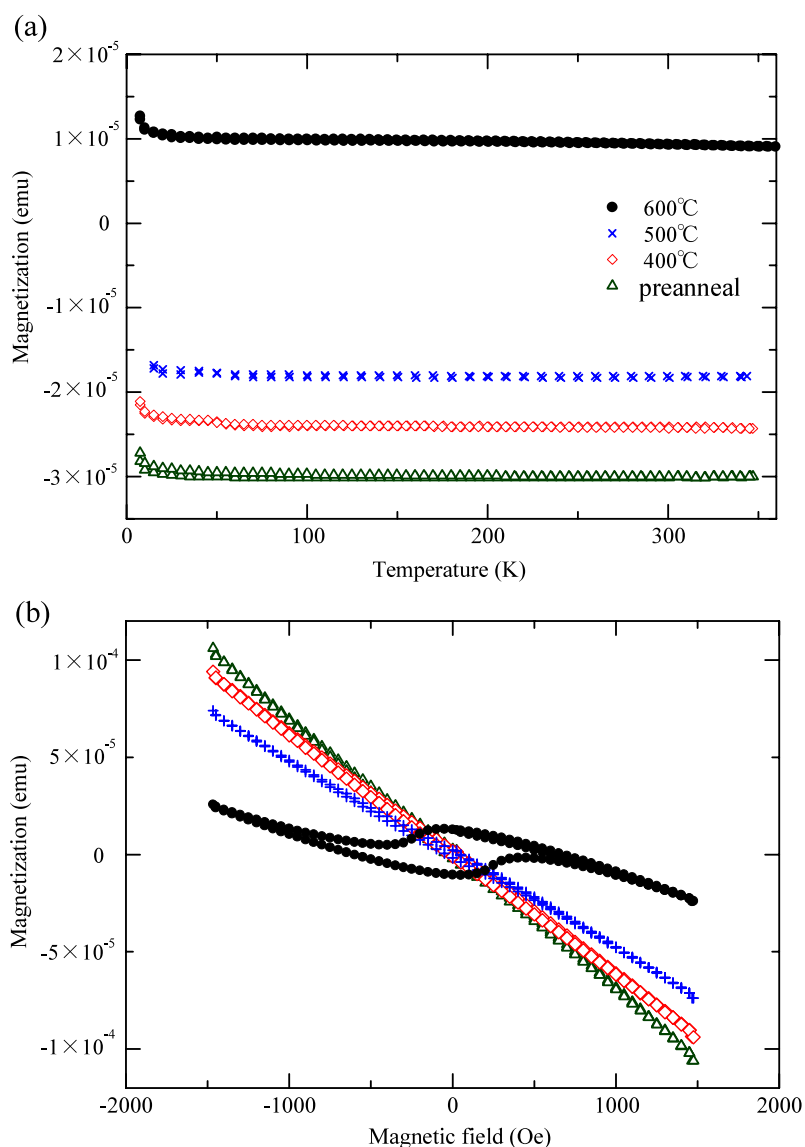


Figure 3. Temperature dependence of magnetization (a) and hysteresis curves (b) for ZnO:5% V films, against the annealing temperature of the RTA for as-deposited films and ones following RTA at 400, 500 and 600 °C.

600 °C, a relatively small hysteresis curve is observed. This is caused by the existence of a very limited ferromagnetic region or canted spins in the antiferromagnetic spin coupling. (In the XMCD measurement results of Fujimori *et al*, a small ferromagnetic signal is observed for the ZnO:5% V thin films. Details will be discussed in a report in the near future.)

To understand the origin of the ferromagnetic properties of these samples, we make a division between the intrinsic mechanism and the extrinsic one. In particular, in the case of ZnO:Co films, the ferromagnetic signals coming from metal Co should be neglected. PES spectra do not reveal peaks from metal Co and metal V. Furthermore, visible–UV measurements

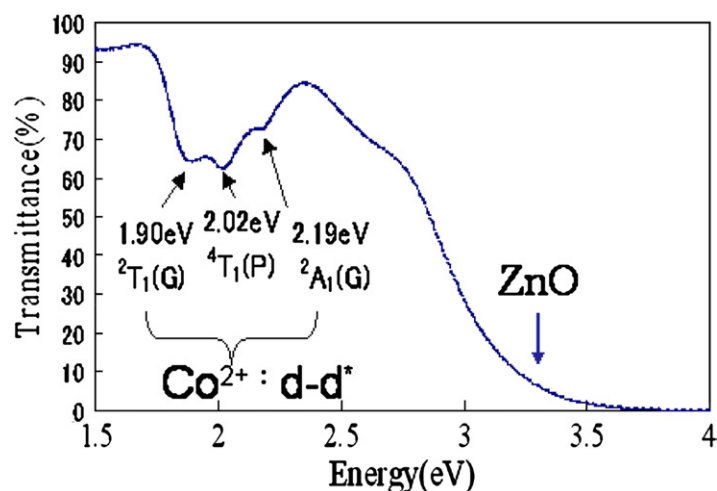


Figure 4. A visible-UV spectrum of ZnO:15% Co film.

for ZnO:Co films show typical absorption spectra corresponding to d-d band absorption of Co^{2+} (figure 4). The ZnO:V films also show characteristic spectral absorption signals located at 560 nm ($\text{V}^{2+}:^4\text{T}_1(\text{e}^2\text{t}^1) \Rightarrow ^4\text{T}_1(\text{e}^1\text{t}^2)$) and 850 nm ($\text{V}^{2+}:^4\text{T}_1(\text{e}^2\text{t}^1) \Rightarrow ^4\text{A}_2$). From these results, we infer that both Co and V ions have 2+ states in the ZnO films.

SQUID results show the ferromagnetic properties of Co-doped ZnO films above room temperature, both in our measurements and in those obtained by our collaborators. So reproducible ferromagnetic properties are confirmed. But we still have a problem as regards the reproducibility and the fluctuation of the magnetic moment from 0.1 to 0.3 μ_{B}/Co . Inhomogeneity of the substituted transition metal ions and/or carrier concentration may be the cause(s).

Moreover, research on the magnetism of transition-metal-doped ZnO on sapphire substrate has also met with success, and the magnetic properties have been examined by means of MCD measurements and NMR measurements. In the case of Co-doped ZnO, it is confirmed that there is no other phase in the film up to 15 mol% ($x = 0.15$), by Raman spectra measurements. Spinel phase was observed around $x = 0.30$, and the Co oxides were observed above $x = 0.40$ in XRD measurements. For V-doped ZnO, the Raman spectrum confirms the single phase up to $x = 0.05$. From XRD measurements, the sample seems to be single phase at $x = 0-0.15$, but spinel phase was observed above $x = 0.20$. These results suggest that MCD measurements are effective for checking the impurity phases (figure 5).

The magnetic field dependence of the MCD signal for Co-doped ZnO clearly showed a ferromagnetic hysteresis loop (figure 6(a)), but V-doped ZnO thin film did not show a hysteresis curve, which indicates paramagnetic features (figure 6(b)). Alexander *et al* suggest that the band-gap size depends on the magnetic phase [11]. A blue shift can be observed in the case of antiferromagnetic material; a red shift indicates ferromagnetic material [12, 13]. Thus we have one clear piece of evidence for ferromagnetism.

The position of the MCD peak at Γ critical points plotted against temperature is shown in figure 7. The dashed curve is fitted to the typical paramagnetic properties. A red shift can be seen below 200 K, which means that the ZnO:Co film is ferromagnet with a Curie temperature of 200 K. In contrast, a red shift was not observed for V-doped ZnO in the temperature range of 10-300 K.

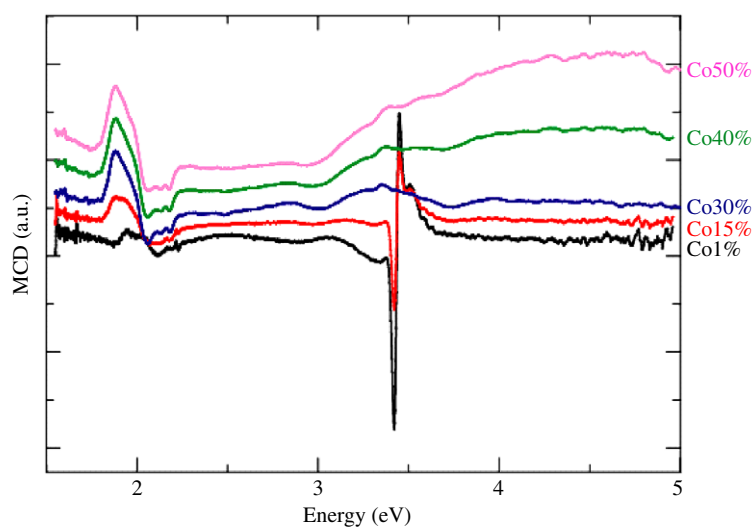


Figure 5. Spectra of the magnetic circular dichroism of ZnO:15% Co films at 10 K.

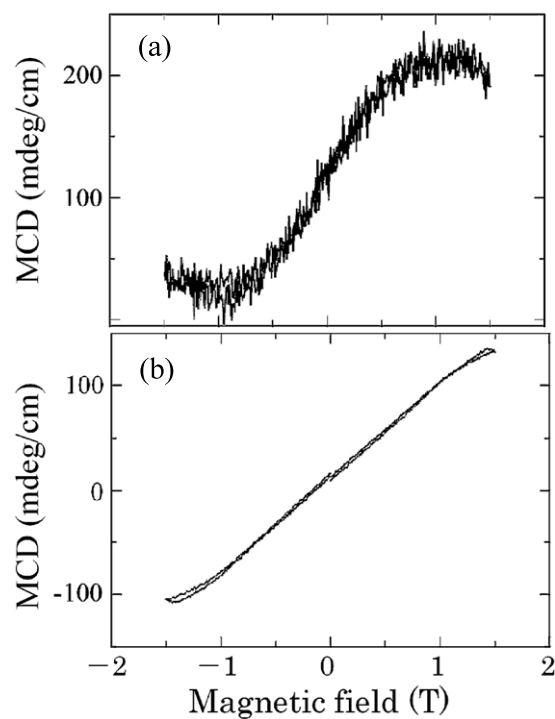


Figure 6. The magnetic field dependence of MCD spectra at 10 K for (a) Co-doped and (b) V-doped ZnO films.

NMR measurements were carried out for the ZnO:Co films. The measurements were done at 4.2 K, a frequency of 148 MHz and $\tau = 25 \mu\text{s}$. Figure 8 shows a typical NMR signal of Co-doped ZnO thin film. In this measurement, five samples were piled up in order to achieve

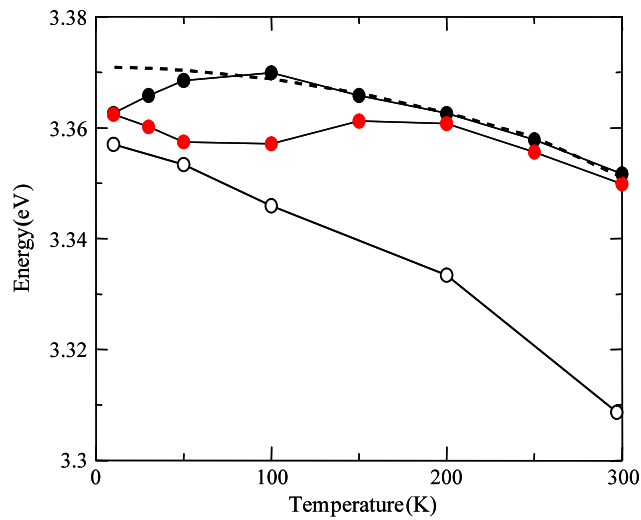


Figure 7. The temperature dependence of the MCD peak.

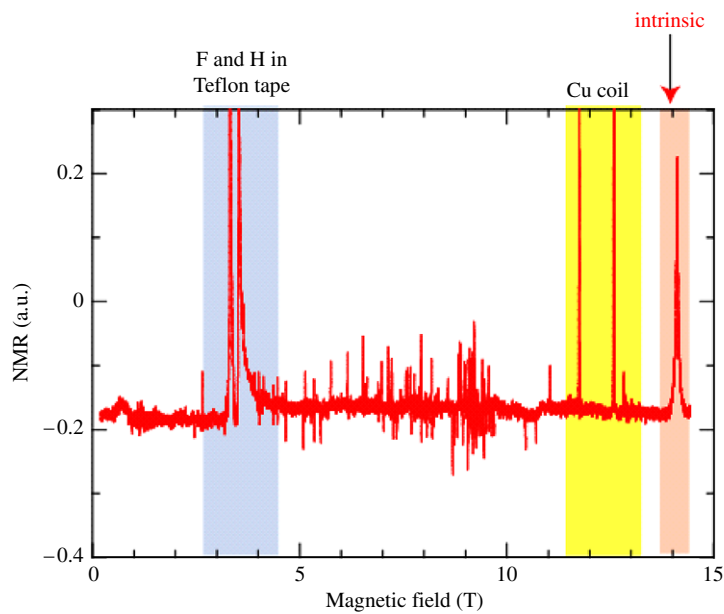


Figure 8. An NMR spectrum of 15% Co-doped ZnO thin film.

volume. The peaks at 3–4 T and 12–13 T arise from the Teflon tape and Cu coil respectively. The sharp peak at 14.1 T is assigned to Co in ZnO. For atomic Co, the value of $h/Bg\mu\gamma$ is 10.03. Therefore, the signal must be at 14.76 T if this sample is paramagnetic. But the observed peak was at around 14.1 T. It turns out that an internal magnetic field of 0.6 T has arisen, suggesting a ferromagnetic signal (figure 8).

4. Conclusion

The fabrication of transition metal substituted ZnO films has been performed. MCD and NMR measurements on Co- and V-doped ZnO thin films on sapphire substrates have been performed. Co-doped ZnO shows ferromagnetic behaviour in both measurements. Although SQUID results suggest ferromagnetic character for V-doped ZnO, the MCD indicates paramagnetic behaviour.

Acknowledgments

The author is grateful to Mr Kobayashi, Mr Ishida and Professor Fujimori who did the XMCD, XAS and PES spectra measurements and to Mr Shiotani and Professors Zheng and Kitaoka who did the NMR measurements.

References

- [1] Dietl T, Ohno H, Matsukura F, Cibert J and Ferrand D 2000 *Science* **287** 1019
- [2] Sato K and Katayama-Yoshida H 2001 *Physica B* **308–310** 904
- [3] Sato K and Katayama-Yoshida H 2001 *Japan. J. Appl. Phys.* **40** 790
- [4] Lee E-C and Chang K J 2004 *Phys. Rev. B* **65** 085209
- [5] Ohno Y, Young D K, Beschoten B, Matsukura F, Ohno H and Awschalom D D 1999 *Nature* **402** 790
- [6] Ueda K, Tabata H and Kawai T 1999 *Appl. Phys. Lett.* **75** 4088
- [7] Saeki H, Tabata H and Kawai T 2001 *Solid State Commun.* **120** 439
- [8] Matsui H, Saeki H, Tabata H and Kawai T 2003 *J. Electrochem. Soc.* **150** G508
- [9] Matsui H, Saeki H, Tabata H and Kawai T 2003 *Japan. J. Appl. Phys.* **42** 5494
- [10] Joseph M, Tabata H, Saeki H, Ueda K and Kawai T 2001 *Physica B* **302/303** 140–8
- [11] Alexander S 1975 *Phys. Rev. B* **13** 304
- [12] Ando K 1992 *Phys. Rev. B* **46** 12289
- [13] Diouri J 1985 *Phys. Rev. B* **31** 7995